Journal of Applied Polymer Science

Mechanical/optical behaviors of imogolite hydrogels depending on their compositions and oriented structures

Kazuhiro Shikinaka, Yumi Koizumi, Kiyotaka Shigehara
Graduate School of Engineering, Tokyo University of Agriculture and Technology, 2-24-16, Naka-cho, Koganei, Tokyo, 184-8588, Japan
Correspondence to: K. Shigehara (E-mail: jun@cc.tuat.ac.jp)

ABSTRACT: A robust acrylamide (AAm) hydrogel reinforced by imogolite (IG), a perfect rigid nanotubular clay mineral, exhibited distinct tensile stress–strain characteristics and strain-induced birefringence in accordance with the compositions of the gels. The gel showed a reversible anisotropic/isotropic structural transition in response to stretching/releasing before the breakdown strain. The strain-induced birefringence of the IG-reinforced gels could be fixed by the in situ interpenetrating polymerization of other AAm monomers that were impregnated into the gels in the stretched states. This resulted in gels with nonvolatile anisotropic birefringence, and therefore, the fixed anisotropic IG ordering showed specific stress–strain characteristics depending on the orientation of IG.
 J. Appl. Polym. Sci. **2015**, *132*, 41691.

KEYWORDS: clay; gels; mechanical properties; nanotubes; optical properties

Received 18 August 2014; accepted 28 October 2014
DOI: 10.1002/app.41691

INTRODUCTION

The industrial and biomedical application of hydrogels, made of either natural or synthetic sources, are usually limited by their poor mechanical properties due to their inhomogeneous structure.[1–4] In recent decades, various kinds of novel hydrogels with high mechanical strength and well-defined structures due to unique molecular designing have been developed.[5–7] Previously, we have also succeeded in obtaining robust hydrogels that showed strain responsible structural ordering by the addition of imogolite (later denoted as IG), a rigid hollow inorganic nanotube, as a nanofiller.[8,9]

IG is a single-walled alumino-silicate nanotubular clay mineral with the composition of $(HO)_3Al_2O_3SiOH$ and an extremely high aspect ratio[10–15]: the external and internal diameters are approximately 2 and 1 nm, respectively; by contrast, the length ranges from sub to several micrometers. Since IG is a perfectly rigid polyelectrolyte,[16,17] it has been used as a constituent of inorganic–organic nanocomposites.[18–20] The outer and inner surfaces of IG are covered with $Al(OH)_2$ and Si(OH) groups, respectively. Because these groups act as the proton-capturing and -releasing functions, respectively, the charge density of IG surfaces varies with the pH and ionic strength of aqueous media. Due to these properties, the dispersibility of IG in water changes drastically depending on the pH, that is, IGs disperse as thin bundles or even monofilaments in acidic and relatively low ionic strength aqueous media (pH $\approx$ 4) to yield opaque to transparent solutions. However, they aggregate into thick bundles or networks and yield apparently turbid dispersions with an increase in pH and/or ionic strength.[21] It has also been reported that amine molecules smaller than the internal diameter of IG nanotubes can be trapped in the hollows due to the interaction with acidic Si(OH) groups.[17,22–24]

In our present research, freshly synthesized IGs were sonicated in pure water to obtain slightly opaque solutions with IG concentration of 6.4 w/v%. These IG nanotubes gave robust hydrogels (later denoted as IG gels) by the *in situ* radical polymerization of a vinyl monomer, acrylamide (AAm).[8,9] The resulting IG gels exhibited a distinct reversible isotropic–anisotropic structural transition in response to small tensile strain. These results encourage us to use of IGs for an attainment of high mechanical strength and well-ordered structure of hydrogels.

In this article, we examine the relationship between the component balance and the mechanical/optical properties of the IG gels by means of tensile strain testing and polarized optical microscopy. According to the experimental results of our research, a mechanism for strengthening AAm gel by the addition of IG nanotubes is discussed. Furthermore, we attempted to fix the resultant anisotropic ordering of IG nanotubes under tensile strain via the formation of an interpenetrating polymer network (IPN) for an addition of nonvolatile anisotropic mechanical/optical properties to IG gels.

EXPERIMENTAL

Chemicals

Deionized water was further purified by a Milli-Q® Advantage A10® system (Millipore™, Eschborn, Germany) and used throughout our experiments. Acrylamide (AAm; Junsei Chemical Co., Ltd., Japan) as a monomer and *N,N′*-methylenebis(acrylamide) (MBAA; Tokyo Kasei Co., Ltd., Japan) as a crosslinking agent were recrystallized from chloroform and ethanol. 4,4′-azobis(4-cyanovaleric Acid) (ACVA; Wako Junyaku Co., Ltd., Japan), as an initiator, $AlCl_3{\cdot}6H_2O$ (Kanto Chem. Co. Inc., Japan), Na_4SiO_4 (Junsei Chem. Co. Ltd., Japan), and other reagent grade chemicals were used as received.

Imogolite (IG) Synthesis

The literature procedure[9,20] was modified in order to easily obtain homogeneously dispersive IGs. Aqueous solutions of $AlCl_3 \cdot 6H_2O$ (9.96 g in 369 mL) and Na_4SiO_4 (6.90 g in 362 mL) were mixed to prepare a solution containing 12.5 and 2.5 mol/L of Al and Si, respectively. The pH of the mixture was adjusted to 6.0 by *rapidly* adding about 26 mL of 1.0 mol/L NaOH aq. (localized high pH levels should be avoided by vigorous agitation), and the resulting solution was stirred for 1 h. The white precipitates were collected by centrifugation and were then redispersed in 400 mL of water with stirring. After the addition of another 2400 mL of water, the solution was acidified (pH = 4.5) by adding 1.0 mol/L hydrochloric acid (7–8 mL), and then stirred at 100°C *continuously* (should not be intermittent) for 4 days. After cooling to room temperature, a fine powder of sodium chloride (16.4 g) was added to the solution with rapid agitation, and the resulting gel was collected by centrifugation (5000 rpm, 30 min) and then washed portionwise with 500 mL water on a 100 nm Millipore filter with suction. The wet products (caution, never allow to dry) were added to 1800 mL of tetrahydrofuran (THF; without stabilizer) with stirring, and the resulting fluffy precipitates were collected by filtration and dried *in vacuo*, resulting in a yield of 42%.

Preparation of PAAm Gels Containing IG (IG Gels) by *In Situ* Polymerization

The literature procedure[9,20] was modified for the present synthesis. A calculated amount of IG in pure water was sonicated for 4 h at 100 W at room temperature (FU-21H, SD-ULTRA. Ltd, KOREA), which was maintained by the occasional addition of ice into the sonicator bath. By this procedure, slightly opaque solutions up to 5.5 w/v% could be prepared, and the average length of IG in the solution was shortened to 131 nm, as estimated from transmission electron microscopy. AAm (2.0 or 4.0 mol/L), MBAA (0, 0.1, or 1.0 mol % vs. AAm), and ACVA (0.1 mol % vs. AAm) were added to IG (1.0 or 5.0 w/v%) aqueous solution or pure water under N_2 atmosphere. The mixtures were placed in the polymerization cells, consisting of a pair of glass plates with 1.0 mm silicon film spacers. After the radical polymerization at 60°C for 24 h, the resulting PAAm gels containing IG were equilibrated by immersing them in running pure water for a week.

Preparation of IG Gels with Fixed Anisotropic Ordering

The gels prepared above were further equilibrated in 1.0 mol/L AAm + ACVA (0.1 mol % vs. AAm) aq. for a week and were stretched by applying the tensile strain of 2 mm/mm to induce the anisotropic ordering of IG nanotubes. While maintaining the strain, the gels were heated at 60°C for 24 h to obtain the post-polymerized gels carrying interpenetrated PAAm chains, after first being equilibrated by immersing them in running pure water for a week.

Transmission Electron Microscopy (TEM)

TEM observations were performed using a JEM-2100 (JEOL, Tokyo, Japan) at an acceleration voltage of 200 kV. About 5 μL of the sample solution was dropped on to carbon-coated grids (Oken Shouji Co., Tokyo), whose surface had previously been turned hydrophilic by glow discharge under reduced pressure. After 3 min, the sample on the grids was blotted by a filter paper, and then the grid was dried in ethanol vapor atmosphere according to the sample preparation method described in a previous study.[25] The digital TEM data were obtained using a slow-scan charge-coupled device (CCD) camera (Gatan USC1000, Gatan Inc.) and converted into images with a frame size of 1024 × 1024 pixels. A cold finger and a cold trap cooled with liquid nitrogen were used to prevent sample contamination by the electron beams. The length of the IG nanotubes was calculated from the TEM images using a DigitalMicrograph® (Gatan Inc.).

Water Content Determination of Gels

The water content of the gels cut into approximately 5.0 × 5.0 × 1.5 mm was determined using a heater-type moisture analyzer (MS-70, A&D Co. Ltd., Japan).

Tensile Measurement of Gels

For tensile testing, the gels were cut into dumbbell-shaped test pieces standardized by JIS-K6251-7 (length 35 mm, width 6 mm, thickness ~2 mm, gauge length 12 mm, inner width 2 mm) with a cutting machine (Dumb Bell Co., Ltd). The sample length between two chucks was 15–20 mm. The tensile stress–strain measurements were performed on a tensile-compressive tester (Tensilon RTC-1310A, Orientec Co.) at a constant stretch rate of 100 mm/min. All measurements were carried out at ambient temperature (22°C ± 2°C) under a relative humidity (RH) of about 60%.

Birefringence Estimation of Gels

The center points of the dumbbell-shaped samples described above were observed at room temperature by a polarized optical microscope (POM; BX51, Olympus, Japan) under crossed nicols. The images were obtained using a CCD camera (Olympus, Japan). The birefringence, Δn, was measured from the retardation values using a Berek compensator (U-CBE, Olympus, Japan). The birefringence of gels during elongation was measured by POM after fixing the two ends of the sample on a vernier caliper and elongating it to a given strain. All measurements were carried out at ambient temperature (22°C ± 2°C) under RH of about 60%.

RESULTS AND DISCUSSION

Preparation of IG

When the IGs purified by reprecipitation from THF were sonicated for 4 h in pure water, their average length decreased to 131 nm (Figure 1), and a slightly opaque solution with IG concentration of 6.4 w/v% was obtained. Compared with the general preparative method of freeze-drying, this procedure allows

a much easier preparation of IG solutions, as the final stage of purification only needs prolonged sonication for 12 h to obtain an identically concentrated aqueous solution and results in a shorter IG's average length of 69 nm.[9]

Preparation and Characterization of IG Gels

Water-soluble molecules bearing amine, amide, or related functionalities have been known to interact with the IG's acidic inner Si(OH) residues if the molecules are small enough to penetrate into the hollows of the IG nanotubes.[17] Therefore, we noted that the mere aqueous mixture of IG and *preformed* PAAm gave no gels, because it is very difficult for the PAAm macromolecular strands to penetrate into the hollows. However, according to our previous study,[9] the *in situ* polymerization of the monomeric AAm in the presence of IG, that is, IG/AAm in pure water, gave robust hydrogels (later denoted as IG gels). Based on the experimental fact that the *in situ* polymerized IG/AAm system without the crosslinking agent, MBAA, gave IG gels, we concluded that the mouth of each IG hollow anchored a few PAAm strands to play a pseudo-crosslinking role. Such gels obtained by *in situ* polymerization with or without MBAA showed birefringence only upon stretching due to the strain-induced uniaxial alignments of IG nanotubes via shear inducing. Herein, to estimate the distinct relationship between the mechanical/optical properties and the composition of IG gels, we measured the stress–strain curves and the birefringence (Δn) changes as a function of the strain applied to the IG gels with various IG, MBAA, and AAm compositions. The names of the gels such as "IG5/L0/AAm4" or "IG5/L0.1/AAm4" represent,

IG5 w/v%/cross**L**inker (=MBAA) **0** mol % vs. AAm/**AAm4** mol/L or
IG5 w/v%/cross**L**inker (=MBAA) **0.1** mol % vs. AAm/**AAm4** mol/L,
respectively.

As described, because the IG nanotubes play the role of pseudo-crosslinking agents, the mechanical strength of the resulting IG gels of IG/L0/AAm4 are drastically reduced with decreasing IG content from IG5 to IG1, in terms of both the modulus and breakdown stress/strain [Figure 2(a)]. In Figure 2(b), the birefringence change with increasing strain is illustrated. A bell-shaped curve is seen with the IG5/L0/AAm4 gel. Since the AAm units are known to give a negative birefringence change upon the ordering of PAAm strands by stretching,[9] such as is seen with the IG0/L0.1/AAm4 gel in Figure 2(b), the bell-shaped curve of the IG5/L0/AAm4 gel can be explained by the overlay of the two counter effects. Upon stretching, the IG nanotubes become uniaxially ordered. The birefringence change is very sensitive to this, and even at a relatively small strain of about 3 mm/mm, Δn increases to as high as 7×10^{-5}. This profile suggests that the IG nanotube ordering, enough to influence Δn, began at the very early stage of stain addition. When the IG content decreased, such as with IG1/L0/AAm4, the counter effects balanced and Δn seemed to be unchanged upon stretching. The results are shown in Figure 2 and indicate that the stretching force was transmitted directly to the IG nanotubes through the pseudo-crosslinking points, bringing about the higher orientation of IG nanotubes and resulting in a larger Δn of the IG gels.

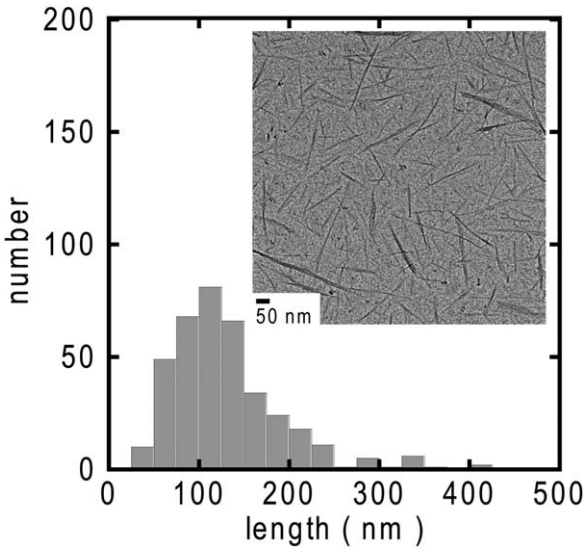

Figure 1. Histograms of the length distributions and TEM image (inserted) of IGs purified by the reprecipitation from THF dispersed in pure water at 5.5 w/v% ($n = 377$).

In order to investigate the difference between the pseudo-crosslinking and the ordinary MBAA crosslinking points, the changes in Δn by stretching were studied at various MBAA contents. As shown in Figure 3(a), the IG gels became brittle with increasing MBAA content or increasing numbers of crosslinking points, because excessive restraints of the IG nanotubes causes inefficient stress dispersion in the PAAm networks of the gels. This tendency is the same as reported previously for similar IG gels.[9] As for the Δn–strain relationship, the IG5/L0.1/AAm4 and IG5/L0/AAm4 gels exhibited similar bell-shaped profiles [Figure 3(b)]. Because the peak values of the two gels were almost the same, the crosslinking points derived by MBAA were not effective in enhancing the degree of IG orientation. The peak top shifts toward smaller strain on increasing the MBAA content from L0 to L0.1. This showed that the crosslinking by MBAA, as well as the pseudo-crosslinking, increased the stiffness of the network [Figure 3(a)] and therefore, assisted the orientation of the IG nanotubes. When the MBAA content is increased to L1.0, the gel becomes hard and brittle, and therefore, the incremental increase in Δn of the IG5/L1.0/AAm4 gel is interrupted at a relatively small strain.

As usually seen in ordinary PAAm gels, the modulus and breakdown stress/strain become smaller with decreasing AAm content in the IG5/L0/AAm gels [Figure 4(a)]. The average mouth-to-mouth distance of two adjacent IG nanotubes, d, is estimated to be about 330 nm according to following equation: $d = \left[\left(\frac{\sqrt{2}\pi}{6f}\right)^{1/3} - 1\right] a$, where f and a is the volume fraction of IG (0.0165) and the average length of IG nanotubes (131 nm), respectively. If every mouth of an IG hollow carries two PAAm strands (since two strands can be inserted per hollow) and every PAAm strand interconnects IG hollows in a mouth-to-mouth anchoring style, as illustrated in Figure 4(b), the average

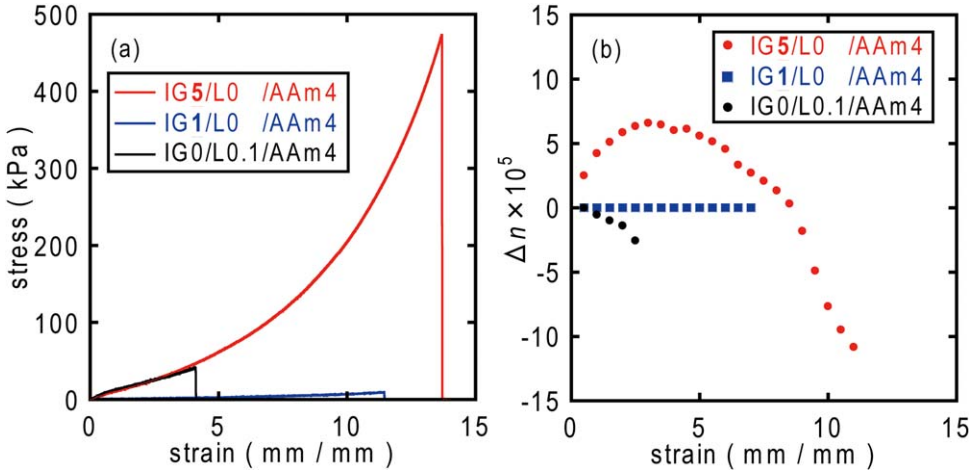

Figure 2. (**a**) Typical tensile stress–strain curves of IG gels with various IG content; IG5/L0/AAm4 (*red line*), IG1/L0/AAm4 (*blue line*, water content 99%), and an ordinary AAm gel (IG0/L0.1/AAm4, *black line*). (**b**) Strain-induced Δn change of IG5/L0/AAm4 (*red circles*), IG1/L0/AAm4 (*blue squares*), and an ordinary AAm gel (IG0/L0.1/AAm4, *black circles*). Measurements were carried out until the gel fractured. [Color figure can be viewed in the online issue, which is available at wileyonlinelibrary.com.]

"stretched" length of PAAm strands is calculated to be about 2300 and 4600 nm in the IG5/L0/AAm2 and IG5/L0/AAm4 gels, respectively, according to the d value and the number of AAm molecules in the gels. Since the interconnection of IG nanotubes by such pseudo-crosslinking through the mouths of hollows might be imperfect and the numbers of PAAm strands anchored to one mouth could be less than 2, it is quite reasonable that these gels can exhibit relatively large strains, such as 11 and 14 mm/mm for IG5/L0/AAm2 and IG5/L0/AAm4, respectively, as illustrated in Figure 4(a). As for the birefringence upon stretching, the Δn value of the IG5/L0/AAm2 gel increases steeply with a small change in tensile strain and is soon saturated to a relatively high value of $\Delta n = 12 \times 10^{-5}$ beyond a strain of 5 mm/mm. In contrast, the strain dependence of Δn in the IG5/L0/AAm4 gel, as illustrated in both Figures 3(b) and 4(c), shows a bell-shaped curve, due to the ordering of the IG nanotubes and PAAm strands. Although the PAAm strands tend to exhibit negative birefringence upon stretching, an ordinary PAAm gel of 2 mol/L (IG0/L0.1/AAm2) never shows birefringence under the strain, due to the low density of AAm units. When the PAAm concentration was increased to 4 mol/L, such as with IG5/L0/AAm4, the high density of the AAm units, as well as the enhanced freedom of the longer polymer strands, allowing easier uniaxial ordering of PAAm upon stretching, lead to a negative Δn in the high strain region. When introducing extra crosslinking points by adding MBAA, as also shown in the results of Figure 3, the gels become stiff and therefore, the stretching becomes ineffective to the Δn change. Overall, upon stretching the IG gels, the IG nanotubes loosely interconnected via pseudo-crosslinking points, as illustrated in Figure 4(b) start

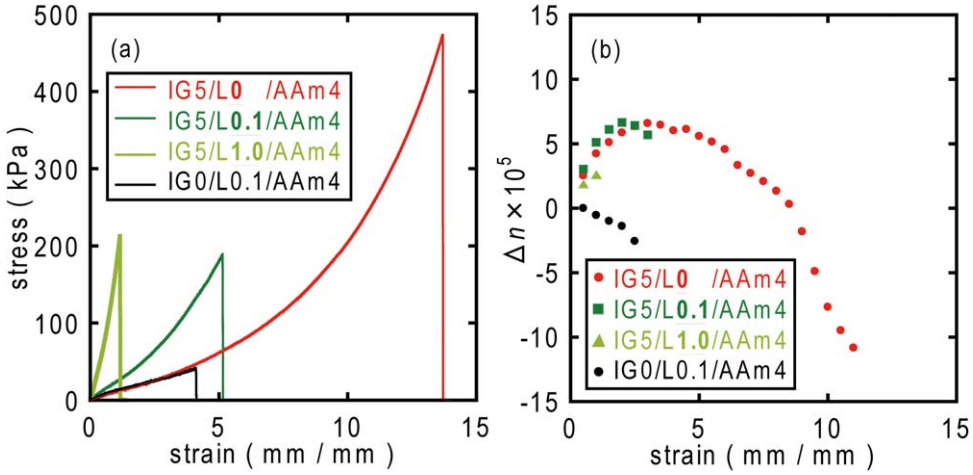

Figure 3. (**a**) Typical tensile stress–strain curves of IG gels with various MBAA content; IG5/L0/AAm4 (*red line*), IG5/L0.1/AAm4 (*dark green line*, water content 92%), IG5/L1.0/AAm4 (*greenish yellow line*, water content 85%), and an ordinary AAm gel (IG0/L0.1/AAm4, *black line*). (**b**) Strain-induced Δn change of IG5/L0/AAm4 (*red circles*), IG5/L0.1/AAm4 (*dark green squares*), IG5/L1.0/AAm4 (*greenish yellow triangles*), and an ordinary AAm gel (IG0/L0.1/AAm4, *black circles*). Measurements were carried out until the gel fractured. [Color figure can be viewed in the online issue, which is available at wileyonlinelibrary.com.]

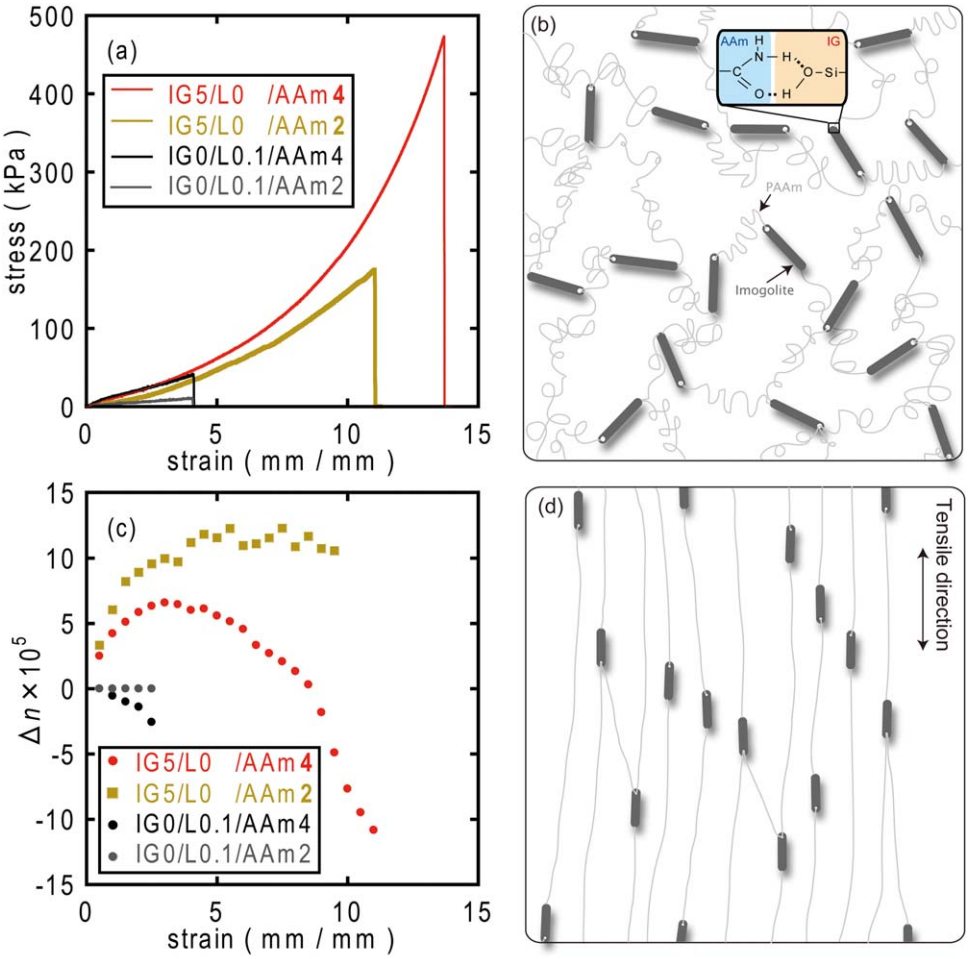

Figure 4. (**a**) Typical tensile stress–strain curves of IG gels with various AAm content; IG5/L0/AAm4 (*red line*) and IG5/L0/AAm2 (*brown line*, water content 96%), and an ordinary AAm gel (IG0/L0.1/AAm4: *black line* and IG0/L0.1/AAm2: *gray line*, water content 96%). (**b**) Schematic illustration of IG gel structures. *In situ* polymerization of AAm in the presence of IGs gives a gel consisting of PAAm network crosslinked by IG. Inserted chemical structure indicates an interaction schemes between AAm and IG. (**c**) Strain-induced Δn change of IG5/L0/AAm4 (*red circles*) and IG5/L0/AAm2 (*brown squares*), and an ordinary AAm gel (IG0/L0.1/AAm4: *black circles* and IG0/L0.1/AAm2: *gray circles*). Measurements were carried out until the gel fractured. (**d**) Schematic illustration of IG gel structures under tensile strain. Applying tensile stress generates the orientation of IGs and PAAm in the gel. [Color figure can be viewed in the online issue, which is available at wileyonlinelibrary.com.]

to order sharply in a single directed alignment, as illustrated in Figure 4(d).

Preparation and Characterization of Oriented IPN Gels

In order to utilize such IG gels as anisotropic materials, the uniform alignment of IG nanotubes and PAAm network (i.e., the strain-induced birefringence) was pinned by entangling other PAAm strands into the aligned IG gels in the style of IPN gels. Figure 5(a) outlines the procedure to fix the uniform alignment in the IG gels. First, the IG5/L0/AAm4 gels are soaked and equilibrated in 1 mol/L AAm aq. for 1 week. Such impregnated IG gels were then laid out under a tensile strain = 2 mm/mm, and the AAm monomers in the gels are post-polymerized while maintaining the tensile strain at 60°C for 24 h for fixation of the elongated IG nanotubes and PAAm chains in the strained gels.

Figure 5(b) shows the POM images of the resulting post-polymerized gels (later denoted as oriented IPN gels) *after the removal of tensile strain and after being equilibrated in water* for 1 week. When the crossed nicols were rotated in respect to the pre-stretched direction as a baseline, a complete extinction was observed at analyzer angles = 0° or 90°, while the maximum brightness was observed at 45°. This result indicates that the IG nanotubes align uniaxially along the pre-stretched direction.[9] Since the IG0/L0.1/AAm4 gels never showed the birefringence even under a tensile strain = 2 mm/mm, the presence of IGs induces such anisotropic birefringence.[9] It was somewhat disappointing that the Δn value of IG5/L0/AAm4 decreased after IPN formation from 5.7×10^{-5} to 1.27×10^{-5}, due to the increased spatial concentration of the negatively birefringent AAm units.

The oriented IPN gels also exhibit anisotropic mechanical properties, as shown in Figure 5(c). Comparing the perpendicular and parallel elongations with respect to the IG orientation or the pre-stretched direction, the maximum breakdown stress and

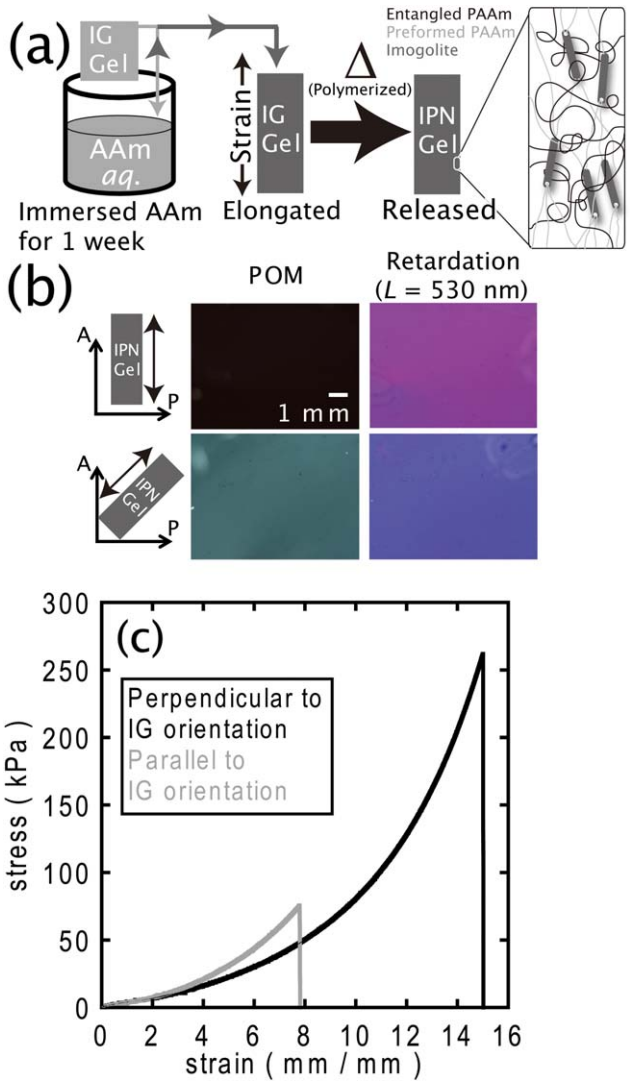

Figure 5. (**a**) Schematic illustration of the procedure to obtain oriented IPN gels. (**b**) POM images of the oriented IPN gel *without tensile strain*. Angle between the gel and analyzer (A)/polarizer (P) is shown on the left-hand side. *Arrows* at the side of the gel illustration indicate the predicted orientation direction of the IG nanotubes in the gels (i.e., tensile direction up to post-polymerization). (**c**) Typical tensile stress–strain curves of the oriented IPN gels (water content: 96%) measured from the perpendicular (*black line*) and parallel (*gray line*) stretching, with respect to the IG orientation. [Color figure can be viewed in the online issue, which is available at wileyonlinelibrary.com.]

strain were larger in the former by a factor of 3.5 and 1.9, respectively.

CONCLUSIONS

This article describes the detailed mechanical/optical properties of AAm gels reinforced by IG nanotubes (IG gels). The tensile stress-strain characteristics and the strain-induced birefringence change of the IG gels are tunable by control of their component balance. Furthermore, the strain-induced birefringence of IG gels can be pinned by entangling another PAAm chain with the IG nanotubes and PAAm network in the gels. The resulting IG gels with a well-oriented structure exhibit robust and anisotropic mechanical properties. Thus, the present experimental system yields gels that are reinforced and functionalized by the nanotubes, and this shows promise in various material applications, such as the fabrication of anisotropic materials.

ACKNOWLEDGMENTS

This work was supported by the JGC-S Scholarship Foundation (No. 1335) and by the JSPS KAKENHI Grant Number 26870179.

REFERENCES

1. Drury, J. L.; Mooney, D. *J. Biomaterials* **2003**, *24*, 4337.
2. Lultolf, M. P.; Hubbell, J. A. *Nat. Biotechnol.* **2005**, *23*, 47.
3. Calvert, P. *Adv. Mater.* **2009**, *21*, 743.
4. Derossi, D.; Kajiwara, K.; Osada, Y.; Yamauchi, A. In Polymer Gels; Plenum: New York, **1991**.
5. Okumura, Y.; Ito, K. *Adv. Mater.* **2001**, *13*, 485.
6. Gong, J. P.; Katsuyama, Y.; Kurokawa, T.; Osada, Y. *Adv. Mater.* **2003**, *15*, 1155.
7. Yang, W.; Furukawa, H.; Gong, J. P. *Adv. Mater.* **2008**, *20*, 1.
8. Shikinaka, K.; Koizumi, Y.; Osada, Y.; Shigehara, K. *Polym. Adv. Technol.* **2011**, *22*, 1212.
9. Shikinaka, K.; Kaneda, K.; Koizumi, Y.; Osada, Y.; Masunaga, H.; Shigehara, K. *Polymer* **2013**, *54*, 2489.
10. Cradwick, P. D. G.; Farmer, V. C.; Russell, J. D.; Masson, C. R.; Wada, K.; Yoshinaga, N. *Nat. Phys. Sci.* **1972**, *240*, 187.
11. Bursill, L. A.; Peng, J. L.; Bourgeois, L. N. *Philos. Mag. A* **2000**, *80*, 105.
12. Mukherjee, S.; Bartlow, V. M.; Nair, S. *Chem. Mater.* **2005**, *17*, 4900.
13. Levard, C.; Masion, A.; Rose, J.; Doelsch, E.; Borschneck, D.; Dominici, C.; Ziarelli, F.; Bottero, J.-Y. *J. Am. Chem. Soc.* **2009**, *131*, 17080.
14. Farmer, V. C.; Adams, M. J.; Fraser, A. R.; Palmieri, F. *Clay Miner.* **1983**, *18*, 459.
15. Farmer, V. C.; Fraser, A. R.; Tait, J. M. *J. Chem. Soc. Chem. Commun.* **1977**, *13*, 462.
16. Donkai, N.; Inagaki, H.; Kajiwara, K.; Urakawa, H.; Schmidt, M. *Makromol. Chem.* **1985**, *186*, 2623.
17. Harsh, J. B.; Traina, S. J.; Boyle, J.; Yang, Y. *Clays Clay Miner.* **1992**, *40*, 700.
18. Yamamoto, K.; Otsuka, H.; Wada, S.; Sohn, D.; Takahara, A. *Soft Matter* **2005**, *1*, 372.
19. Yang, H.; Chen, Y.; Su, Z. *Chem. Mater.* **2007**, *19*, 3087.
20. Shikinaka, K.; Kaneda, K.; Mori, S.; Maki, T.; Masunaga, H.; Osada, Y.; Shigehara, K. *Small* **2014**, *10*, 1813.
21. Karube, J. *Clays Clay Miner.* **1998**, *46*, 583.
22. Imamura, S.; Hayashi, Y.; Kajiwara, K.; Hoshino, H.; Kaito, C. *Ind. Eng. Chem. Res.* **1993** *32*, 600.
23. Bonelli, B.; Bottero, I.; Ballarini, N.; Passeri, S.; Cavani, F. *J. Catal.* **2009**, *264*, 15.
24. Henmi, T.; Wada, K. *Clay Miner.* **1974**, *10*, 231.
25. Yang, H.; Su, Z. *Chin. Sci. Bull.* **2007**, *52*, 2301.